

⟨Review Article⟩

## **Malate dehydrogenase of *Geobacillus stearothermophilus*: A practically feasible enzyme for clinical and food analysis**

Yuya Shimozawa<sup>1</sup> and Yoshiaki Nishiya<sup>1</sup>

**Summary** Malate dehydrogenase (MDH) is used in the diagnostic assay for aspartate aminotransferase activity and determination of serum bicarbonate level. The enzyme is also used in assays for determination of L-malate and acetate in food products. The structure and catalytic mechanism of MDH are highly similar to those of lactate dehydrogenase (LDH). The efficiency of mutated LDH of *Geobacillus stearothermophilus* that is converted to MDH was investigated for the assays. However, the utilization for the assays was discontinued because of two main disadvantages, stringency of substrate specificity and dependence on allosteric effector. On the other hand, the development of a thermostable MDH from *G. stearothermophilus* (gs-MDH) was successful and the enzyme is now in commercial use. In contrast to the mutated LDH, gs-MDH exhibited a high substrate specificity and no allosteric effect. Detailed comparison of the enzymatic properties of gs-MDH and other commercially available MDHs demonstrated the highest substrate affinity and stability of gs-MDH, which were desirable in diagnostic reagents. To investigate the evolution of MDH and LDH, orthologues from several bacterial genome sequences were investigated. Results of homology search suggested drastic structural changes in MDH in comparison to those in LDH, probably due to difference in metabolic roles. The catalytic loop of MDH containing the active site histidine was highly conserved among gs-MDH and MDHs of other moderate thermophiles. The efficiency of gs-MDH in the assays was verified by simple simulations of sequential enzyme reactions, based on their kinetic parameters. Simulations results also paved the way to improve the feasibility of gs-MDH for use in other assays.

**Key words:** Malate dehydrogenase, Lactate dehydrogenase, Substrate specificity, Aspartate aminotransferase, Bicarbonate

---

<sup>1</sup>Division of Life Science, Graduate School of Science and Engineering, Setsunan University, 17-8 Ikeda-Nakamachi, Neyagawa, Osaka 572-8508, Japan.

To whom correspondence should be addressed.

Dr. Yoshiaki Nishiya

Division of Life Science, Graduate School of Science and Engineering, Setsunan University, 17-8 Ikeda-Nakamachi, Neyagawa, Osaka 572-8508, Japan.

Fax: +81-72-838-6599

E-mail: nishiya@lif.setsunan.ac.jp

Received for Publication: Aug 2, 2019

Accepted for Publication: Aug 22, 2019

## 1. Fundamentals and applications of malate dehydrogenase

Malate dehydrogenase (EC 1.1.1.37; L-malate: NAD<sup>+</sup> oxidoreductase, abbreviated MDH) catalyzes the reversible reduction of oxaloacetate to L-malate, using reduced β-nicotinamide adenine dinucleotide (NADH) as a coenzyme. This enzyme exhibits a sequential ordered Bi Bi reaction mechanism with NADH as the first substrate and oxaloacetate as the second (Fig. 1A). MDH is a key enzyme in the TCA cycle and plays important metabolic roles in aerobic energy-production pathways. MDH is useful for the clinical determination of aspartate aminotransferase (AST, also known as glutamate oxaloacetate transaminase) activity<sup>1</sup> and bicarbonate levels<sup>2</sup> in serum by coupling with related reagents. MDH is also utilized in the determinations of L-malate and acetate in various food products<sup>3,4</sup>.

As for application of MDH, structural information is necessary to fully understand the enzymatic properties. Crystal structures of apo and substrate-bound forms of MDHs have revealed movement of the binding loop structures around the substrate binding pocket<sup>5</sup>. The motion of the binding loops might play a key role in substrate binding and subsequent enzyme activity. A close-up view of the active site region of oxaloacetate-bound MDH<sup>6</sup> is shown in Fig. 1B. One histidine (H) and three arginine (R) residues were conserved in each of the

MDHs. The imidazole group of H acts as an acid base catalyst. The side chains of two R, which coordinate with the carboxy groups of oxaloacetate, are important for substrate binding and specificity. Structural differences among MDHs were observed around two large flexible loops (catalytic loop and mobile loop) at the entrance to the active site (Fig. 1B)<sup>6</sup>.

The three-dimensional structure and catalytic mechanism of MDH are highly similar to lactate dehydrogenase (EC 1.1.1.27; L-lactate: NAD<sup>+</sup> oxidoreductase, abbreviated LDH), which catalyzes the reversible reduction of pyruvate to L-lactate, using NADH as a coenzyme. Evolutionary analyses of MDH and LDH demonstrated that the enzymes are closely related<sup>7</sup>. The structure-function relationship of MDH and LDH has previously been studied by X-ray crystallographic analyses and protein engineering<sup>8-15</sup>. Site-directed mutagenesis studies showed that LDH can be easily converted to MDH by substituting only one amino acid in the substrate-binding site [glutamine (Q) to R]. However, this LDH-based MDH was not a practical alternative for the clinical assays.

In this review, development of MDH from the moderately thermophilic bacterium *Geobacillus stearothermophilus* (abbreviated gs-MDH) as a practically feasible enzyme is described. Structural analysis and reaction simulation of MDH for application to the clinical and food assays are also

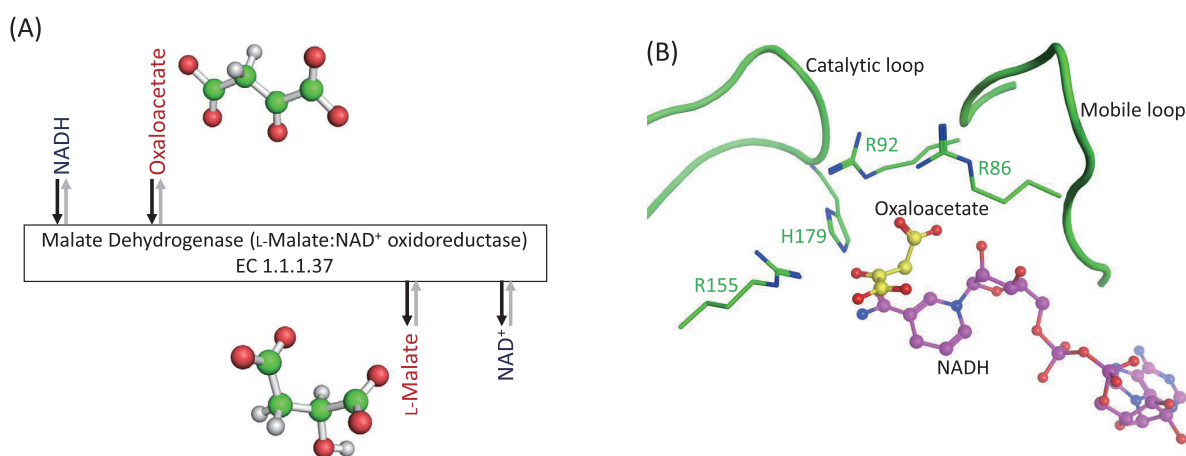


Fig. 1 Enzymatic reaction and structure of MDH. (A) MDH reaction. Hydrogen, carbon, and oxygen of substrate and product are represented by white, green, and red balls, respectively. (B) Close-up view of the active site region of MDH.

explained. Enzymes from moderate thermophiles, such as the genus *Geobacillus*, exhibited sufficient stability as diagnostic enzymes. Especially, they have a high preservation stability and an acceptable reactivity at 30-37, which are necessary conditions for liquid diagnostic reagents. However, the *Geobacillus* MDH has not been industrially used, presumably due to the spread of mammalian MDH as a de facto standard.

## 2. Development of gs-MDH

The MDHs from *Sus scrofa* (pig) mitochondria and *Thermus flavus* (extremely thermophilic bacterium), abbreviated as pm-MDH and tf-MDH, respectively, were commercially produced and utilized as diagnostic reagents<sup>11,12</sup>. These warranted further improvements in substrate affinities and preservation stabilities in the diagnostic reagent for AST. Hence, the efficiency of mutated LDH from *G. stearothermophilus* converted to MDH (gs-LDH\_Q102R)<sup>8</sup> was investigated for application to the

assays. gs-LDH is commercially available<sup>16</sup> and is utilized for the clinical determination of alanine aminotransferase activity in serum by coupling with related reagents<sup>1</sup>. Therefore, the mutant gs-LDH was also expected to be practically feasible for the AST assay reagents. However, the utilization of gs-LDH\_Q102R was discontinued because of two main disadvantages, stringency of substrate specificity and dependence on allosteric effector (Table 1).

On the other hand, the development of gs-MDH, which is a thermostable MDH from *G. stearothermophilus*, was successful. The gene was cloned and effectively expressed in *Escherichia coli*<sup>17</sup>. The enzyme of the recombinant strain was purified to homogeneity by a simple process (Fig. 2). In contrast to gs-LDH\_Q102R, gs-MDH exhibited a high substrate specificity and no detectable activity with pyruvate (Table 1). It exhibited no allosteric effect, like other well-known MDHs. gs-MDH is now in commercial use<sup>18</sup>.

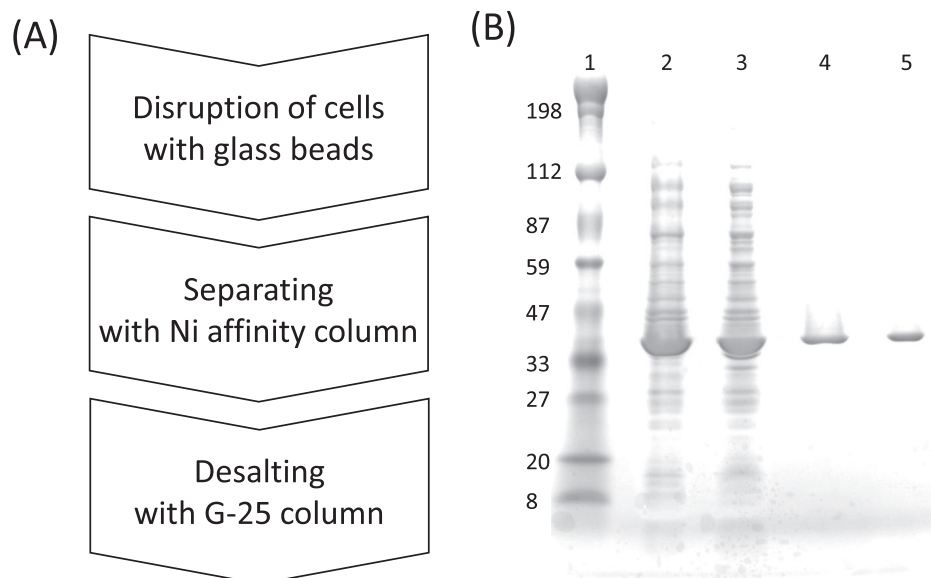


Fig. 2 Purification flow of gs-MDH and SDS-PAGE analysis of each purification process. (A) Purification flow. Recombinant cells were disrupted by rotation of 3,000 rpm with glass beads using Micro smash™ (TOMY) at 4°C for 120 s. Soluble cell extract was purified using an Ni affinity column chromatography (His GraviTrap, GE Healthcare). gs-MDH was eluted by the elution buffer [300 mM imidazole, 500 mM NaCl, and 20 mM potassium phosphate buffer (pH 7.4)]. The purified fractions were desalted by 20 mM potassium phosphate buffer (pH 7.4) using G-25 gel filtration (GE Healthcare). (B) SDS-PAGE analysis. 1: Molecular weight marker, 2: soluble cell extract, 3: insoluble cell extract, 4: eluate of affinity chromatography, 5: eluate of gel filtration.

Table 1 Comparison of gs-LDH mutant and gs-MDH

Enzyme	$K_m$ for oxaloacetate ( $\mu\text{mol/L}$ )	Substrate specificity (pyruvate/oxaloacetate) ( $k_{cat}$ , %)	Allosteric effector
gs-LDH_Q102R	19	1.2	D-fructose 1,6-diphosphate
gs-MDH	5.0	not detected	none

Table 2 Comparison of commercially available MDHs

Enzyme	$K_m$ for oxalo- acetate ( $\mu\text{mol/L}$ )	Optimal temperature ( $^{\circ}\text{C}$ )	Optimal pH	Thermal stability ( $^{\circ}\text{C}$ )	Stability (powder) (y)	Remaining activity in AST assay reagent after 7 d at $40^{\circ}\text{C}$ (%)
gs-MDH	5.0	70	8.0	$\leq 70$	5	94
pm-MDH	33	50	8.0	$\leq 30$	nt	nd
tf-MDH	68	90	8.0	$\leq 70$	nt	85

Temperature activity, in 0.1 mol/L potassium phosphate buffer (pH 7.5); pH activity, in 0.1 mol/L buffer solution (pH 5-8, phosphate; pH 8-9, borate) at  $25^{\circ}\text{C}$ ; nt, not tested. Thermal stability, 15 min-treatment with 0.1 mol/L potassium phosphate buffer (pH 7.5). AST assay reagent contained 5 U/mL malate dehydrogenase, 0.5 U/mL lactate dehydrogenase, 175 mmol/L L-aspartate, 30 mmol/L  $\alpha$ -ketoglutarate, 0.22 mmol/L NADH, 0.1 mmol/L pyridoxal phosphate, and 50 mmol/L PIPES buffer (pH 7.4). Reproduced with permission from the Society of Analytical Bio-Science<sup>6</sup>.

### 3. Comparison of enzymatic properties

The detailed enzymatic properties of commercially available MDHs, including the  $K_m$  values for oxaloacetate and temperature and pH profiles, were investigated and compared with one other (Table 2)<sup>6</sup>. The  $K_m$  of gs-MDH was much lower than those of the other enzymes, i.e., the enzyme exhibited the highest substrate affinity. gs-MDH also had a high optimum temperature for application as a diagnostic enzyme, usually  $37^{\circ}\text{C}$ , although that of tf-MDH was much higher. The temperature stability of gs-MDH was the same as that of tf-MDH but much greater than that of pm-MDH. The gs-MDH, tf-MDH, and pm-MDH activities remaining after storage at  $40^{\circ}\text{C}$  for 1 week were estimated as 94%, 85%, and 0%, respectively. Accordingly, gs-MDH exhibited the highest stability as the diagnostic reagent for AST. These properties of gs-MDH make it ideal for clinical applications. The powder form of lyophilized gs-MDH is commercially available and stable for at least 5 years.

### 4. Primary structural analysis of gs-MDH

Enzyme structure provides a reasonable starting point for analysis of the structure-function relationship. The gs-MDH sequence (DDBJ/EMBL/GenBank accession number: LC100138) provided information for evolution and function of MDH/LDH family by comparing with other primary structures. It was also deemed useful as a base for homology modeling of gs-MDH.

To discuss evolutionary process of MDH and LDH, orthologues from five representative genome sequences of gram-positive bacteria and a phototrophic bacterium (*G. stearothermophilus*, *Bacillus subtilis*, *Halobacillus halophilus*, *Corynebacterium glutamicum*, and *Chloroflexus aurantiacus*) were investigated. Results of homology search suggested drastic structural changes in MDH in comparison to those in LDH, probably due to difference in their roles in metabolism (Fig. 3A). For example, the amino acid sequence of gs-MDH was 21.5-87.0% identical to that of four other MDHs. In contrast,

(A)

	MDH (Gst)	MDH (Bsu)	MDH (Hha)	MDH (Cgl)	MDH (Cau)	LDH (Gst)	LDH (Bsu)	LDH (Hha)	LDH (Cgl)	LDH (Cau)
MDH (Gst)		87.0	83.2	21.5	57.7	<u>36.0</u>	35.2	33.5	35.0	31.5
MDH (Bsu)	87.0		80.7	22.9	56.0	35.9	<u>35.8</u>	33.8	33.5	33.2
MDH (Hha)	83.2	80.7		nh	54.5	35.4	35.1	<u>33.9</u>	33.9	33.0
MDH (Cgl)	21.5	22.9	nh		nh	26.7	19.3	20.8	nh	23.2
MDH (Cau)	57.7	56.0	54.5	nh		30.6	32.5	28.5	31.3	<u>32.1</u>
LDH (Gst)	<u>36.0</u>	35.1	35.4	19.1	30.6		<b>69.0</b>	<b>65.0</b>	<b>60.3</b>	<b>47.6</b>
LDH (Bsu)	35.2	<u>35.8</u>	34.9	19.3	32.5	<b>69.0</b>		<b>64.6</b>	<b>58.1</b>	<b>45.0</b>
LDH (Hha)	33.5	33.8	<u>33.9</u>	20.8	28.5	<b>65.0</b>	<b>64.6</b>		<b>56.3</b>	<b>48.6</b>
LDH (Cgl)	35.0	33.7	33.9	nh	31.3	<b>60.3</b>	<b>58.1</b>	<b>56.3</b>		<b>45.9</b>
LDH (Cau)	31.5	33.2	33.0	23.2	<u>32.1</u>	<b>47.6</b>	<b>45.0</b>	<b>48.6</b>	<b>45.9</b>	

nh: no homology

(B)

	173	Active site ↓	185	Homology with gs-MDH (%)
<i>Geobacillus</i>	-G-F-V-L-G-G-H-G-D-D-M-V-P-			100
<i>Parageobacillus</i>	-G-F-V-L-G-G-H-G-D-D-M-V-P-			96.8
<i>Bacillus</i>	-G-F-V-L-G-G-H-G-D-E-M-V-P-			84.8
<i>Brevibacillus</i>	-G-F-V-L-G-G-H-G-D-D-M-V-P-			80.0
<i>Thermobacillus</i>	-G-F-V-L-G-G-H-G-D-D-M-V-P-			74.4
<i>Sulfobacillus</i>	-A-F-V-M-G-G-H-G-D-D-M-V-P-			61.8
<i>Chloroflexus</i>	-A-M-L-M-G-G-H-G-D-E-M-V-P-			57.7
<i>Acidithiobacillus</i>	-A-M-V-L-G-E-H-G-D-G-I-V-P-			23.9
<i>Mycolicibacterium</i>	-M-T-I-W-G-N-H-S-A-T-Q-Y-P-			19.5

Fig. 3 Comparison of MDH amino acid sequences. (A) Homology matrix for MDH and LDH sequences. Gst, Bsu, Hha, Cgl, and Cau exhibit the origins of sequences (*G. stearothermophilus* ATCC12016, *B. subtilis* 168, *H. halophilus* HBHAL\_3757, *C. glutamicum* ATCC13032, and *C. aurantiacus* Caur\_1675, respectively). Homologies between MDHs and between LDHs were shown by dark grey (outline character) and light grey (bold), respectively. Homologies between MDH and LDH of the identical origins were underlined. (B) Multiple alignment of partial MDH sequences from *G. stearothermophilus* ATCC12016, *Parageobacillus thermoglucosidasius* DSM2542, *B. subtilis* 168, *Brevibacillus brevis* BBR47\_13910, *Thermobacillus composti* Theco\_2612, *Sulfobacillus acidophilus* DSM10332, *C. aurantiacus* Caur1675, *Acidithiobacillus ferrooxidans* ATCC53993, and *Mycobacterium phlei* MPHLCUG\_04022. The 13 amino acid sequences adjacent to the active site histidine were compared. Each total homology score with gs-MDH is also shown.

amino acid sequence of gs-LDH exhibited relatively similar homologies with those of other LDHs (47.6-69.0% identities). Moreover, comparison between the sequences of MDH and LDH in the same strains did not show high similarities ( $\leq 36\%$  identity). These results indicated the difference in evolutionary

rates of both enzymes, although these three-dimensional structures were highly similar to each other. Most likely, the mutation frequencies of LDHs were much lower than those of MDHs, due to maintenance of their allostericity. As a result, only the important parts for catalytic mechanism were

conserved regardless of bacterial species. Accordingly, both MDH and LDH should not be evolutionarily compared at the same time.

On the other hand, the catalytic loop of MDH containing the active site residue H was highly conserved among gs-MDH and other moderate thermophiles (Fig. 3B).

### 5. Tertiary structural analysis of gs-MDH

To enhance understanding of the properties of gs-MDH, open (apo) and closed (substrate-bound) molecular models were constructed by homology modeling using base structures with higher sequence identities<sup>6</sup>. The open and closed forms of gs-MDH superimpose well, with a root mean square deviation for atomic C $\alpha$  positions (RMSD) of 1.3 Å. However, the specific region composed of the amino acid residues in the mobile loop, which was predicted to be structurally changed by binding of substrate, exhibited higher RMSD of above 3.0 Å (Fig. 4).

As expected, the three-dimensional structures of gs-MDH are similar to those of other MDH/LDH family enzymes. The enzyme is composed of two domains, a catalytic and an NADH-binding domain. Three R residues, at positions 86, 92, and 155, play an important role in substrate binding (Fig. 1B). The relative spatial positions of residues R86 and R92

change considerably in the open and closed structures, whereas the catalytic residue H179 moves only minimally. R86 and R92 effectively create a positively charged cavity that stabilizes the carboxyl group of oxaloacetate by electrostatic interactions (Fig. 1B).

The unique enzymatic properties of the enzyme, such as thermal stability and substrate affinity, were elucidated based on these structural comparisons<sup>6</sup>. For example, the difference in thermal stability could be understood at the structural level, since gs-MDH contains a considerably larger predicted number of hydrogen bonds than MDH of *B. anthracis*, which is a typical mesophilic enzyme. On the other hand, the distance between the catalytic and mobile loops was small in the closed form of gs-MDH, consistent with the enzyme's high substrate affinity. The active site spaces of the closed forms of gs-MDH and pm-MDH were also compared, and the active site of pm-MDH was wider than that of gs-MDH<sup>6</sup>.

### 6. Application and simulation of gs-MDH for assays

The excellent feasibility of gs-MDH for applications to AST, bicarbonate, L-malate, and acetate assays (Fig. 5) was verified by simple simulations of sequential enzyme reactions, based on their kinetic

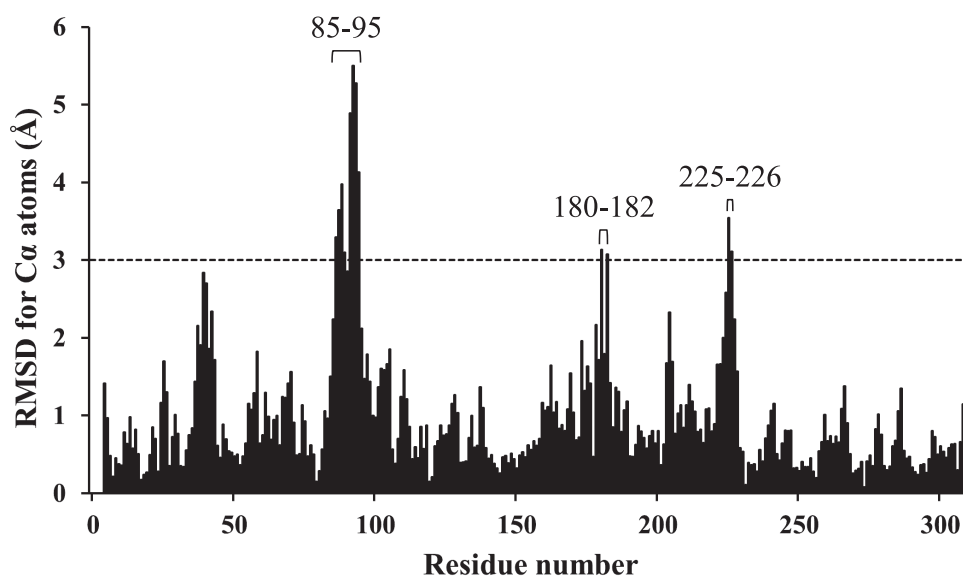


Fig. 4 Comparison of RMSD between open and closed form of gs-MDH homology models. The dashed line was drawn at 3.0 Å. Amino acid residues with higher RMSD of >3.0 Å are shown by numbers.

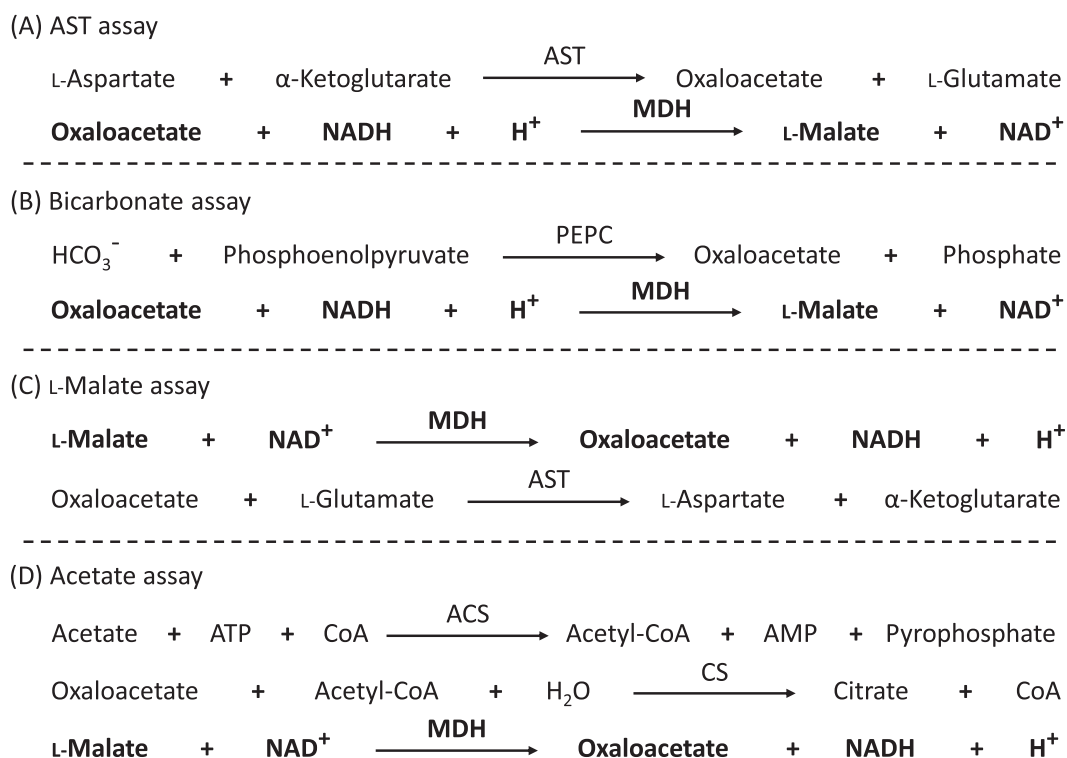


Fig. 5 Principles of MDH-used enzyme assays. (A) Aspartate aminotransferase (AST) assay. AST activity in the sample is measured by following the MDH reaction. (B) Bicarbonate assay. The amount of bicarbonate in the sample is measured by the reactions of phosphoenolpyruvate carboxylase (PEPC) and MDH. (C) L-Malate assay. The amount of L-malate in the sample is measured by MDH. AST is also used to prevent the reverse reaction of MDH. (D) Acetate assay. Acetate in the sample is converted to citrate by the reaction of acetyl-CoA synthetase (ACS) and citrate synthetase (CS). Oxaloacetate is the substrate of CS and produced by MDH. Therefore, the amount of acetate is quantified by increase in the absorbance of NADH by the MDH reaction.

parameters.

As shown in Fig. 6, rate assays of AST with pm-MDH, tf-MDH, and gs-MDH were simulated using Microsoft Excel to examine the influence of substrate affinity on the enzymatic assays. Increase in the levels of oxaloacetate and decrease in the levels of NADH were characterized based on Michaelis-Menten kinetics. Both amounts and concentrations were calculated every 0.1 s. Simple evaluations of the sequential enzyme reactions demonstrated the excellent feasibility of gs-MDH for the AST assay. The estimated minimum level of gs-MDH required was markedly lower than that of the other enzymes. To obtain the same results, approximately one-fifth or less amount of gs-MDH is required as compared with pm-MDH or tf-MDH, in agreement with the  $K_m$  values of enzymes.

Bicarbonate assays were also simulated based on Michaelis-Menten kinetics. To obtain the same

assay results, approximately one- or less of gs-MDH would be required compared with pm-MDH or tf-MDH (Fig. 6). Similarly, enzymatic assay simulations showed that gs-MDH could be useful for clinical and food analysis. Results of the simulations also paved the way to improve the feasibility of gs-MDH for use in each assay or others such as immunoassays and sensors, based on their kinetic parameters.

As described in this review, gs-MDH is considered excellent for applications in the clinical and food analysis in terms of the enzymatic properties, such as stability and reactivity. In fact, this enzyme has already been used in various applications<sup>1-4</sup>. However, MDH has several structurally unclear points, such as the mechanism of conformational change in open and closed forms. Further research is warranted to resolve these issues.

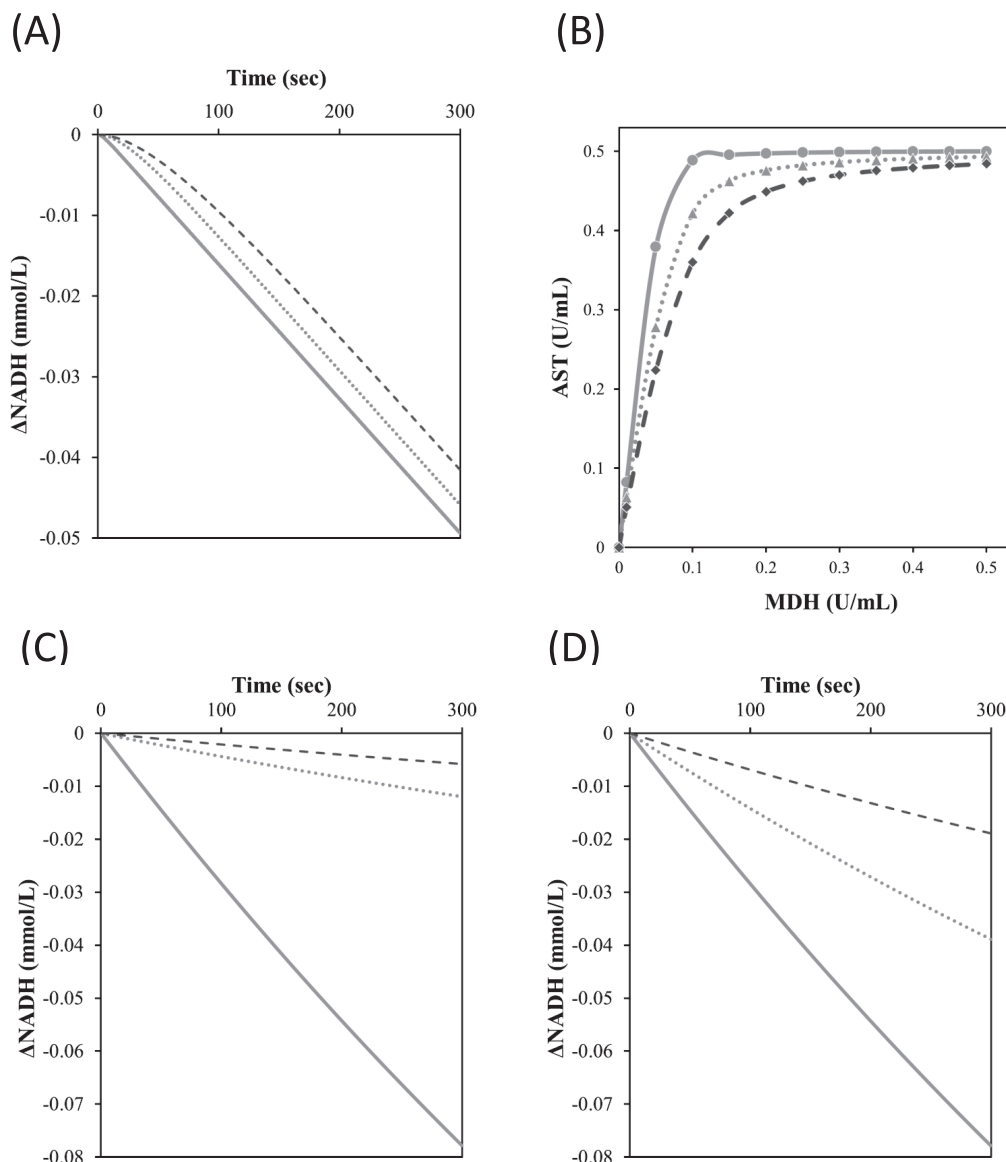


Fig. 6 Simulations of assays. (A and B) Simulations of the rate assays of AST with gs-MDH (solid line), pm-MDH (dotted line), and tf-MDH (dashed line). Decreases in the amount of NADH were simulated every 0.1 s using Microsoft Excel. (A) Comparison of time courses of AST assays. The assay reagents (270  $\mu$ L) containing various concentrations of enzyme and the sample (30  $\mu$ L) were mixed and incubated at 30°C and pH 7.5 for 5 min. Both of the assumed MDH and AST activities were 0.1 U/mL. (B) Dose-response curves of MDHs in the assay reagents. The assumed AST activity in the sample was 0.5 U/mL and MDH activity in the assay reagent was plotted every 0.05 U/mL. (C and D) Simulations of the rate assays of bicarbonate with gs-MDH (solid line), pm-MDH (dotted line), and tf-MDH (dashed line). Decreases in the amount of NADH were simulated every 0.1 s using Microsoft Excel. The assay reagent (40  $\mu$ L) containing various concentrations of enzyme, the sample (2  $\mu$ L) and water (160  $\mu$ L) were mixed and incubated at 30°C and pH 7.5 for 5 min. The expected level of bicarbonate in the sample was 30 mmol/L. The assumed PEPC and MDH activities in the assay reagents were 1 U/mL and 5 U/mL (C) or 50 U/mL (D). Reproduced with permission from the Society of Analytical Bio-Science<sup>6</sup>.

References

1. Wilkinson JH, Baron DN, Moss DW, and Walker PG: Standardization of clinical enzyme assays: A reference method for aspartate and alanine transaminases. *J Clin Pathol*, 25: 940–944, 1972.
2. Peled N: An enzymic bicarbonate reagent that is free of pyruvate interference. *Clin Chem*, 27: 199-200, 1981.



3. Chemnitz GC and Schnid RD: L-Malate determination in wines and fruit juices by flow injection analysis adaptation of a coupled dehydrogenase/transferase system. *Anal Lett*, 22: 2897-2913, 1989.
4. Guynn RW and Veech RL: Enzymatic determination of acetate. *Methods in Enzymol*, 35: 302-307, 1975.
5. Goward CR and Nicholli DJ: Malate dehydrogenase: A model for structure, evolution, and catalysis. *Protein Sci*, 3: 1883-1888, 1994.
6. Nishiya Y and Shimozawa Y: Properties of *Geobacillus stearothermophilus* malate dehydrogenase used as a diagnostic reagent and its characterization by molecular modeling. *Int J Anal Bio-Sci*, 4: 21-27, 2016.
7. Golding GB and Dean AM: The structural basis of molecular adaptation. *Mol Biol Evol*, 15: 355-369, 1998.
8. Wilks HM, Hart KW, Feeney R, et al.: A specific, highly active malate dehydrogenase by redesign of a lactate dehydrogenase framework. *Science*, 242: 1541-1544, 1988.
9. Kallwass HKW, Luyten MA, Parris W, et al.: Effects of Gln102Arg and Cys97Gly mutations on the structural specificity and stereospecificity of the L-lactate dehydrogenase from *Bacillus stearothermophilus*. *J Am Chem Soc*, 114: 4551-4557, 1992.
10. Kallwass HKW, Hogan JK, Macfarlane ELA, et al.: On the factors controlling the structural specificity and stereospecificity of the L-lactate dehydrogenase from *Bacillus stearothermophilus*: Effects of Gln102Arg and Arg171Trp/Tyr double mutations. *J Am Chem Soc*, 114: 10704-10710, 1992.
11. Kelly CA, Nishiyama M, Ohnishi Y, Beppu T, and Birktoft JJ: Determinants of protein thermostability observed in the 1.9-Å crystal structure of malate dehydrogenase from the thermophilic bacterium *Thermus flavus*. *Biochemistry*, 32: 3913-3922, 1993.
12. Chapman AD, Cortes A, Dafforn TR, Clarke AR, and Brady RL: Structural basis of substrate specificity in malate dehydrogenases: crystal structure of a ternary complex of porcine cytoplasmic malate dehydrogenase, alpha-ketomalate and tetrahydroNAD. *J Mol Biol*, 285: 703-712, 1999.
13. Yin Y and Kirsch JF: Identification of functional paralog shift mutations: Conversion of *Escherichia coli* malate dehydrogenase to a lactate dehydrogenase. *Proc Natl Acad Sci USA*, 104: 17353-17357, 2007.
14. Hung CH, Hwang TS, Chang YY, Luo HR, and Wu SP: Crystal structures and molecular dynamics simulations of thermophilic malate dehydrogenase reveal critical loop motion for co-substrate binding. *PLoS One*, 8: e83091, 2013.
15. Kalimeri M, Girard E, Madern D, and Sterpone F: Interface matters: The stiffness route to stability of a thermophilic tetrameric malate dehydrogenase. *PLoS One*, 9: e113895, 2015.
16. Hogan JK, Carlos A. Pitto CA, Jones JB, and Gold M: Improved specificity toward substrates with positively charged side chains by site-directed mutagenesis of the L-lactate dehydrogenase of *Bacillus stearothermophilus*. *Biochemistry*, 34: 4225-4230, 1995.
17. Nishiya Y and Hirayama N: Molecular modeling and substrate binding study of the *Bacillus stearothermophilus* malate dehydrogenase. *J Anal Bio-Sci*, 23: 117-122, 2000.
18. TOYOBO ENZYME HOMEPAGE, [http://www.toyobo.co.jp/seihin/xr/enzyme/pdf\\_files/201707/MAD\\_211.pdf](http://www.toyobo.co.jp/seihin/xr/enzyme/pdf_files/201707/MAD_211.pdf) (accessed 2019.8.20)